ORIGIN AND GENESIS OF CALCRETE IN THE MURRAY BASIN

L.N. Tylkowski., D.J. Chittleborough & K.M. Barovich

CRC LEME, School of Earth and Environmental Sciences, University of Adelaide, SA, 5005

INTRODUCTION

The Murray Basin is a shallow intracratonic sedimentary basin composed of a Cainozoic sedimentary succession that reaches a maximum thickness of 600 m in the central region (Brown & Stephenson 1991). Sedimentation was initiated with the separation of Antarctica and the southern margin of Australia (Cande & Mutter 1982) and is part of the Murray Sequence that extends from the Tertiary to the Present. Calcretes and other regolith carbonate accumulations occur extensively throughout the Murray Basin.

It is widely accepted, although untested by new tracer techniques, that the source of the carbonate is aeolian. In many areas it is referred to as Crocker's Loess. The form and nature of the carbonates is a matter of much speculation. Firman (1964, 1967) and others (e.g., Wetherby & Oades 1975) have assigned various carbonate layers to particular stratigraphic units based on morphology. They have not given consideration to *in situ* processes that may have implications for various carbonate morphologies.

AIMS

The aims of this project are to investigate the genesis of calcrete in relation to the other surrounding units and to determine the difference or similarity between the origins of the various carbonate morphologies. Specifically we test the hypothesis that weathering and translocation processes are responsible for the morphologies of carbonates.

PROFILE & GEOLOGY

The selected profile is situated in South Australia approximately 80 km from Adelaide and 5 km east of the township of Sedan. This corresponds to the far western region of the Murray Basin and occurs within a large area of mappable calcrete (Thompson 1969; Qca). The 271 cm thick profile contains three basic stratigraphic units: the Blanchetown Clay; Quaternary calcretes (including the Ripon and Bakara); and, uppermost Woorinen Formation (Figure 1).

The Blanchetown Clay appears as a red/brown, silty clay that has strong ped development. This Pliocene-Late Pleistocene unit was deposited under fluvio-lacustrine conditions as part of an extensive inland body called Lake Bungunnia (Firman 1965). A transitional zone marks the beginning of a series of calcretes that appear throughout a majority of the profile. These calcretes encompass a variety of morphologies including nodular, indurated, brecciated, laminated and powdery. After a horizon of undifferentiated white indurated carbonate a section of 17 cm of Ripon calcrete is present (Figure 1). Firman (1967) defined that this calcrete is older than the overlying nodular Bakara Calcrete.

The genesis of these calcretes is thought to be due to a contribution of aeolian

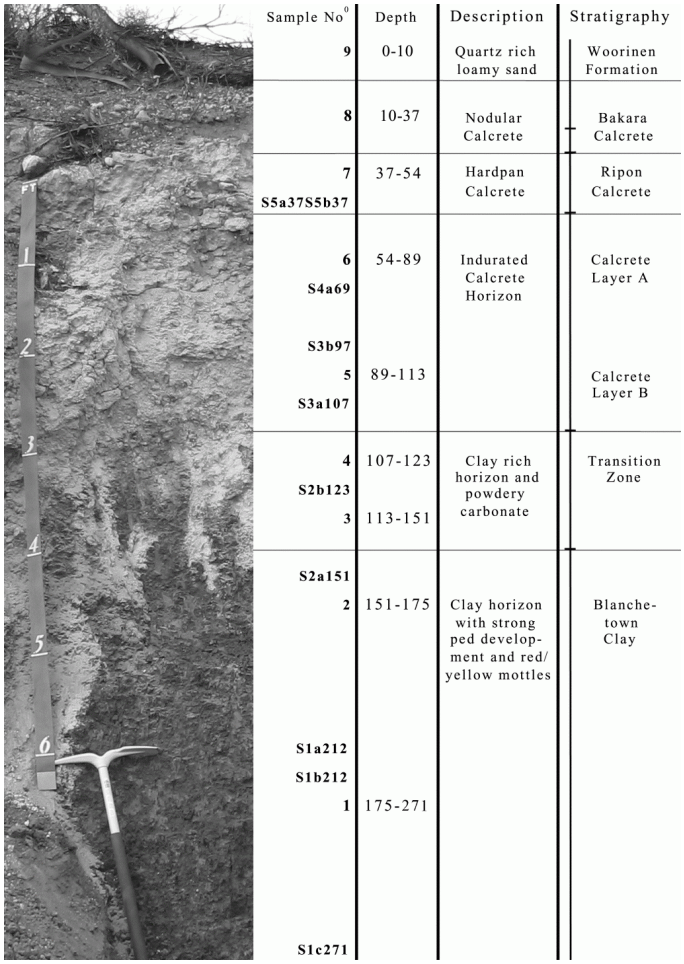

Figure 1: Profile showing sample sites, depth (cm), geological description and known stratigraphy. All samples starting with "S" are at the appropriate depth. Stratigraphic nomenclature collated from Firman (1967, 1972) and Thomson (1969).

deposition followed by leaching of carbonate and finally recrystallisation in the dry matrix of subsurface horizons. However groundwater activity and lateral movement of calcium is another hypothesis that has not been seriously considered. Wetherby & Oades (1975) studied a number of calcretes within the Woorinen Formation and concluded that they formed in a more humid climate with inactive and vegetated dunes. These conditions led to the development of a calcrete horizon by *in situ* soil forming processes.

The above lying unconsolidated dark brown sandy Woorinen Formation is Late Pleistocene with possible Holocene remobilisation (Brown & Stephenson 1991). This unit has undergone pedogenesis with sandy and silty sediments being mixed with clay aggregates and humic material (leaf litter, twigs and rootlets).

METHODS

Particle Size Separation

In the initial process of the geochemical investigation we sieved the samples to separate each bulk sample into two fractions: gravel (> 2 mm); and fine earth (< 2 mm). This measure was taken to separate such horizons as the uppermost Woorinen Formation (Figure 1; sample 9) into nodular calcrete and soil. This process preceded a Particle Size Separation (PSS) which generated five fractions: > 2,000-125 μm (coarse sand), 125-53 μm (fine sand), 53-20 μm (very fine sand) and 20-2 μm (silt) and < 2 μm (clay) (Gee & Or 2002) (Figure 2). This allowed further analysis by Field Emission Secondary Electron Microscopy (FESEM), X-Ray Fluorescence (XRF) and X-Ray Diffraction (XRD) to be specific to certain fractions.

To isolate the residual fractions of the bulk samples (except the Blanchetown Clay), pre-treatment involved the reaction of 1M HCl with approximately 1-1.5 kg of sample to remove mainly carbonates. Organic matter removal was not undertaken as most samples are depleted in organic materials. After drying and weighing a 25 g sample was taken and centrifuged a number of times to remove any soluble salts. The clay (< 2 μm) and silt fraction (2-30 μm) were extracted through aqueous suspension and the remaining sand fraction (20-2,000 μm) was separated into three further fractions (very fine sand, fine sand and coarse sand) by wet sieving using 53 μm and 125 μm grade sieves (Figure 2).

Heavy Mineral Isolation

The fine sand fractions derived from the particle size separation were targeted for this particular technique, as resistant heavy minerals such as zircon and rutile are commonly found in these fractions (Chittleborough 1991). These minerals are considered immobile with respect to vertical displacement and can aid in discriminating between pedogenic and sedimentological changes. Approximately 0.2 g of very fine sand and 0.5 g of fine sand fractions were added to a saturated solution of sodium polytungstate, at a density of 2.9 g/cm^3. After centrifuging for 5 minutes at 3,000 rpm the heavy mineral fraction was extracted by syphoning. Several washings were necessary to dilute the heavy liquid and after drying a portion of sample was syringed onto filter paper and attached to an SEM stub.

Carbon coated samples were examined by a Philips XL30 Field Emission Scanning Electron Microscope (FESEM). Field scans covered a majority of each stub at an accelerating voltage of 15kV, 500x magnification and 10 second elemental count time.

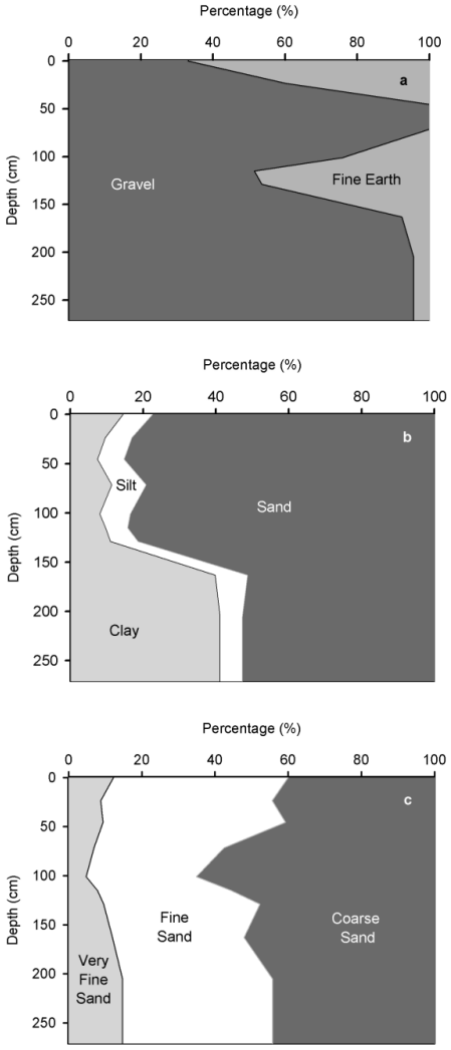

Figure 2: **a**. Original division of bulk sample into gravel (> 2 mm) and fine earth (< 2 mm). Nine samples were taken down the 271 cm profile and results plotted as a percentage. **B**. Particle Size Distribution (PSD) wt. % versus depth (cm) of 50 g of residual fraction from both the fine earth and gravel fractions for samples 9, 8 & 5-1 and from the gravel fraction for samples 7 & 6. All samples were normalised to 100% of the measured value and particle size analyses performed by the methodology of Gee & Or (2002). **c**. Sand particle size distribution of wt. % versus depth (cm) of the collected sand fraction from the PSD. Methodology as per **b**, although sand fractions were separated by wet sieving using a 53 μm and 125 μm sieves.

Fifteen elements were chosen to determine the mineralogy of the grains, including O, Mg, Al, Si, Y, P, Zr, Ti, Ca, La, Ce, Fe, W, Mn and K. For each scan elemental weight percentages (normalized to 100%), position of the grain and dimensions of the grain were recorded.

X-Ray Diffraction (XRD)

X-Ray Diffraction (XRD) analysis was performed on the clay fraction (< 2 μm) only. The mineralogy of this fraction can aid in discriminating between sedimentological and pedogenic processes such as illuviation. Each sample was saturated twice with $MgCl_2$, washed five times with deionized water and five drops of glycerol were added. The samples and membranes were fixed to 32 mm aluminium disks using double sided tape. XRD patterns were collected on a Philips PW1800 microprocessor-controlled diffractometer using Co Kα radiation, variable divergence slit and graphite monochromator. The diffraction patterns were recorded from 3° to 32° 2θ in steps of 0.05° with a 2.0 second counting time per step.

RESULTS & DISCUSSION

The particle size distribution (PSD) (Figure 2) shows similar percentages of sand, silt and clay between the calcretes which differ from the percentages in the Blanchetown Clay. The Blanchetown Clay has an elevated proportion of clay with respect to the calcretes, which are sand rich. The silt fraction remains relatively constant throughout the entire profile. These trends are represented in both the gravel (> 2 mm) fraction and the fine earth (< 2 mm) fraction. Thus there is a similarity between the soil and nodular calcrete within the Woorinen and Bakara Calcrete (Figure 2; depth < 23.5 cm).

The sand particle size distribution shown as Figure 2b illustrates the consistency of the very fine sand (20-53 μm) and fine sand (53-125 μm) fractions throughout the length of the profile. However, there is a moderate increase in both fractions in the Blanchetown Clay, Bakara Calcrete and Woorinen Formation with respect to the other samples. There is an increase in the coarse sand fraction in the middle of the profile within the calcrete layers. Furthermore in most samples an increase or decrease of the 20-53μm fraction is replicated in the 53-125 μm fraction. There are similar results for the gravel and fine earth fractions that demonstrate the similarity between the calcrete and soil within the Woorinen Formation and Bakara Calcrete.

The similarity between the calcrete and soil within the Woorinen Formation is evident within the FESEM scans as samples 9a and 9b have comparable mineralogical distributions (Table 1). FESEM scans of the 20-53 μm show no definitive mineral trends between samples throughout the profile. This result is in contrast to the 53-125 μm fraction which has a similar mineral distribution for samples down the profile until the Blanchetown Clay (Table 1; sample 2b). At this level there is a three to four times increase in zircon, rutile and titanite with ilmenite more than doubled. Within the 53-125 μm fraction there is an overall increase in alumino-silicate minerals within the soil and calcrete horizons and thus lower levels of resistant minerals. Sample 5a shows an increase in iron within this fraction that is not evident within the other calcrete samples. The

Table 1: Mineral Percentages (%) of the heavy mineral (> 2.90 g/cm^3) fraction of the 20-53 μm and 53-125 μm fractions.

#Sample	Depth (cm)	Stratigraphy	Mineral Percentage (%) Al/Si	Fe-O	Ilm	Rut	Zr	Tit	^Other	*Total Grains
20-53μm fraction										
9a	5	Woorinen	48.7	16.7	15.0	7.8	2.6	0.0	8.8	1328
9b	5		55.8	15.9	8.8	6.8	2.1	0.0	10.6	339
8a	23.5	Bakara	36.4	21.0	17.9	8.2	4.0	0.8	11.6	1193
7a	45.5	Ripon	19.7	25.8	21.8	8.9	4.0	1.5	18.2	325
6a	71.5	Calcrete	42.9	22.0	15.2	6.2	2.5	2.4	8.6	787
5a	101		43.5	15.9	16.5	10.5	0.8	2.3	10.4	1119
2b	163	Blanchetown	29.3	19.0	10.8	10.1	1.6	0.9	28.4	744
53-125μm fraction										
9a	5	Woorinen	57.6	6.7	1.3	1.6	0.0	0.0	32.7	373
9b	5		56.1	8.4	1.3	2.4	0.0	0.0	31.6	538
8a	23.5	Bakara	84.7	6.4	3.3	1.3	0.4	0.1	3.9	1661
7a	45.5	Ripon					N/A			
6a	71.5	Calcrete	76.7	12.6	2.4	1.4	0.3	0.0	6.7	1099
5a	101		61.0	21.9	4.4	0.8	0.1	0.2	11.5	1204
2b	163	Blanchetown	36.9	19.3	10.6	8.2	1.4	0.8	22.8	1383

Mineral abbreviations are: Al/Si - alumino silicates; Fe-O - iron oxides; Il – ilmenite; Rut - rutile; Zr - zircon; Zr; and Tit – titanite.

* Total grains counts have been collected by a Philips XL30 Field Emission Scanning Electron Microscope (FESEM) by setting the brightness and contrast to remove contamination by light minerals (< 2.9 g/cm^3) and setting the minimum diameter of grains at 5 μm.

^ Other minerals include contaminated minerals by tungsten from the heavy liquid, undifferentiated mineral assemblages, monazite, xenotime, aluminium oxides and calcite

Samples labelled "**a**" are from the gravel fraction (> 2 mm) and samples labelled "**b**"are from the fine earth fraction (< 2 mm).

Blanchetown Clay is the only sample that has a comparable mineral assemblage between the 20-53 µm and 53-125 µm fractions.

XRD data also illustrates the difference between calcareous horizons and the underlying Blanchetown Clay (Figure 3). Increased concentrations of smectite and randomly interstratified minerals are evident within the Blanchetown Clay as shown by the far left broad peak in Figure 3. Furthermore Figure 3 shows a decrease in illite in the lower calcareous layers shown as the middle peak. However kaolinite is present within all samples and has a consistent relative intensity down the profile.

The FESEM elemental scans of the 53-125 µm fraction demonstrate the change in the proportion of resistant minerals within the Blanchetown Clay with respect to the calcretes. The differentiation of the Blanchetown Clay is reflected within the particle size distribution with an increase in clay within this material and in the XRD data with the presence of smectite. These findings illustrate the sediment-ological difference between the calcrete and the underlying clay. We would suggest the calcretes have precipitated within a geological material other than the Blanchetown Clay. Element concentrations by XRF of all fractions < 2 mm could support this sedimentary change, particularly by calculating the ratio of Zr/Ti down the profile. Furthermore strontium isotope analysis ($^{87}Sr/^{86}Sr$) can determine the source of calcium to the carbonates with respect to each other and the underlying Blanchetown Clay.

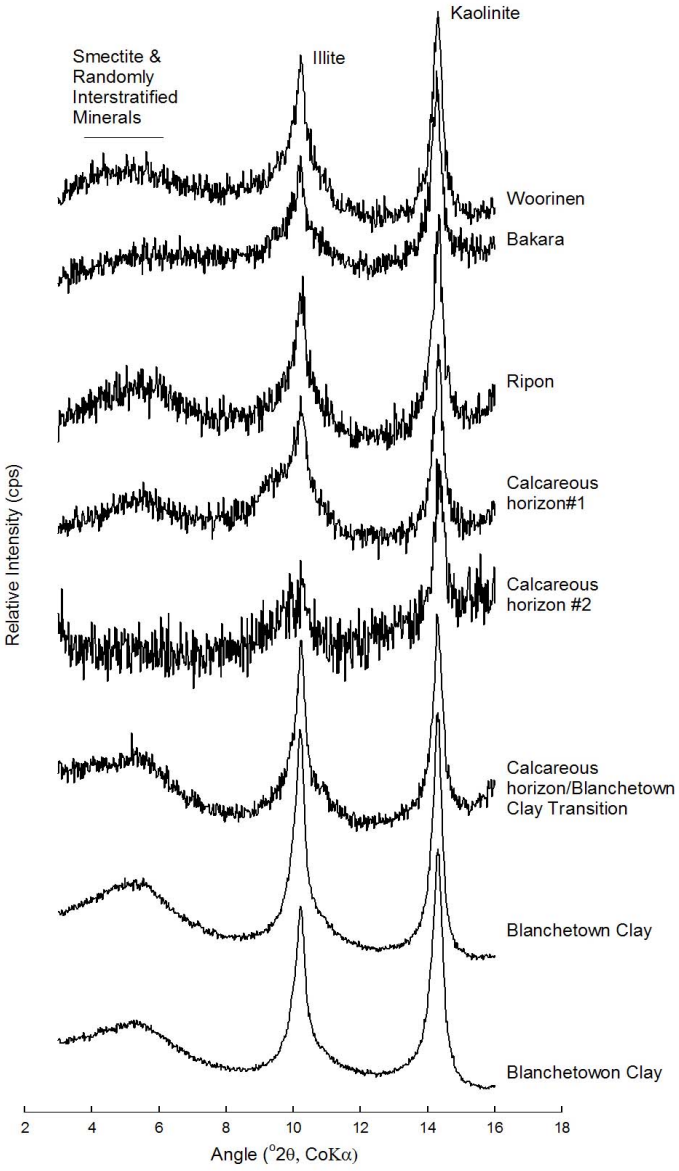

Figure 3: XRD traces of relative intensity versus 2θ angle. All samples from the profile are represented (Figure 1) except 3.

The FESEM elemental scans also illustrate the similarity of resistant minerals between the calcretes. Therefore, if volumetric changes are minimal and extensive illuviation/eluviation processes have not occurred it is likely the calcretes have formed within the same geological material. This finding is contradictory to the Quaternary stratigraphy outlined by Firman (1967) who has separated the calcrete layers as "Bakara", "Ripon" and "Undifferentiated" calcretes. The geol-ogical material for calcrete emplacement is likely to be akin to the Woorinen Formation as both the FESEM elemental scans and PSD show no major difference between the nodular calcrete (Sample 9a; > 2 mm) and quartz rich soil (Sample 9b; < 2 mm) (Figure 2 & Table 1). The morphology of resistant mineral grains such as zircon and rutile by determined by SEM could show a similarity between the soil and nodular calcrete.

The increase in the coarse sand fraction within the Undifferentiated Calcrete layers represented in the sand particle size distribution is unknown (Figure 2). Calcareous layers within the middle of the profile also show a decrease in illite for unknown reasons (Figure 3). This may be a due to the weathering or transport of the finer fractions within this section of the profile or possibly the deposition of differing sediments. The latter hypothesis is improbable as there is no other evidence to indicate differing sediments within the FESEM scans or PSD analysis. However, these hypotheses can be further tested by mass balance calculations based

upon the concentration of Zr and Ti in the 53-125 μm fraction using the method outlined by Brimhall & Lewis (1991). Another unexplained result is the overall higher distribution of resistant minerals (zircon, rutile, titanite) in the 20-53 μm fraction compared with the 53-125 μm fraction and the consistency of mineral assemblages between samples. This homogeneous distribution in the 20-53 μm fraction may be due to the movement of heavy minerals of this particular size throughout the profile or a similar mineral assemblages between sediments.

CONCLUSIONS

Preliminary data illustrates the abrupt sedimentological change between the Blanchetown Clay and the overlying calcrete. We suggest the calcrete horizons have formed within a geological material other than the Blanchetown Clay. As the Blanchetown Clay is a Pliocene-Late Pleistocene deposit, the age of the calcrete is therefore younger than this age. This material is possibly akin to the Woorinen Formation and there is minimal evidence to suggest multiple sediments within the calcrete horizons. However, illuviation/eluviation and weathering processes may have assimilated the geochemical signature of the calcretes, camouflaging sedimentological changes. There are similar proportions of < 2 mm fractions (PSD) and resistant mineral assemblages (FESEM elemental scans) between all calcrete horizons and morphologies. This may indicate a similar age for the calcretes which would contradict the existing stratigraphy outlined by Firman (1967). Further analysis by Sr isotopes, XRF, FESEM and mass balance equations may strengthen or deny this hypothesis. In particular, these analyses could provide a basis for considering whether the various morphologies of calcrete are not indicative of age (therefore stratigraphically separated) but rather particular *in situ* pedological processes.

Acknowledgments: The authors would like to thank Ken Wetherby for providing in depth knowledge of calcretes in the Mallee Region of South Australia. Paul Wittwer, Liam McEntagart and Robert Dart for assistance with field activities. Colin Rivers and David Bruce for assistance in laboratory procedures. CRC LEME and the University of Adelaide for financial support and resources.

REFERENCES

BROWN C.M. & STEPHENSON A.E. 1991. Geology of the Murray Basin, southeastern Australia. *Bureau of Mineral Resources, Geology and Geophysics Bulletin* **235**.

BRIMHALL G.H., LEWIS C.J., FORD C.R.B., BRATT J., TAYLOR G. & WARIN O. 1991. Quantitative geochemical approach to pedogenesis: importance of parent material reduction, volumetric expansion, and eolian influx in lateritization. *Geoderma* **51**, 51-91.

CHITTLEBOROUGH D.J. 1991. Indices of weathering for soils and Palaeosols formed on silicate rocks. *Australian Journal of Earth Sciences* **38(1)**, 115-120.

CANDE S.C. & MUTTER J.C. 1982. A revised identification of the oldest seafloor spreading anomalies between Australia and Antartica. *Earth and Planetary Science Letters* **58**, 151-160.

FIRMAN J.B. 1964. The Bakara Soil and other stratigraphic units of the Late Cainozoic age in the Murray Basin, South Australia. Geological Survey of South Australia, *Quaternary Geological Notes* **10**, 2-5.

FIRMAN J.B. 1965. Late Cainozoic lacustrine deposits in the Murray Basin, South Australia. Geological Survey of South Australia, *Quaternary Geological Notes* **16**, 1-2.

FIRMAN J.B. 1967. Stratigraphy of the Late Cainozoic deposits in South Australia. *Royal Society of South Australia Transactions* **91**, 165-177.

FIRMAN J.B. 1972. *Renmark map sheet*. Geological Survey of South Australia, 1:250,000 Map Series.

GEE G.W. & OR D. 2002. Particle-size analysis *In*: DAWE J.H. & TOPP G.C. eds. *Methods of Soil Analysis Part 4-Physical Methods*. Soil Science Society of America, Madison : Wisconsin USA, pp. 255-289.

THOMSON B.P. 1969. *Adelaide map sheet*. Geological Survey of South Australia, 1:250,000 Map Series.

WETHERBY K.G. & OADES J.M. 1975. Classification of carbonate layers in highland soils of the northern Murray Mallee, South Australia, and their use in stratigraphic and land use studies. *Australian Journal of Soil Research* **13**, 119-132.